JOURNAL OF CATALYSIS 122, 55–67 (1990)

Reactant-Promoted Reaction Mechanism for Catalytic Water–Gas Shift Reaction on MgO

TAKAFUMI SHIDO, KIYOTAKA ASAKURA, AND YASUHIRO IWASAWA

Department of Chemistry, Faculty of Science, University of Tokyo, Hongo, Bunkyo-ku, Tokyo 113, Japan

Received July 10, 1989; revised September 29, 1989

The behavior of reaction intermediates in the catalytic water–gas shift reaction (WGSR) on the MgO surface was studied by means of FT–IR spectroscopy. The hydroxyl groups on top of coordinatively unsaturated Mg atoms reacted with CO to produce three kinds of surface formates of unidentate, bidentate, and bridge types in the order bridge > unidentate > bidentate. Unidentate-type formate was produced at room temperature and decomposed at ca. 450 K. The formation and decomposition of bridge- and bidentate-type formates proceeded at higher temperatures (ca. 400 and 550 K, respectively). In the presence of adsorbed water, unidentate-type formate changed into bridge-type formate and hence most formates are bridge type under reaction conditions. Contrary to previous reports, formate intermediates were never converted to H_2 and CO_2 in the absence of H_2O. While all the formates decompose to CO and surface OH by themselves, adsorbed water promoted the decomposition of formates to the WGSR products H_2 and CO_2 through electronic interaction between the adsorbed water and the formate. The reaction rate of WGSR at steady state agreed with the decomposition rate of the bridge-type formate intermediate to H_2 and CO_2 in the presence of water.

INTRODUCTION

Reaction intermediates, in general, coexist with reactants and products adsorbed on catalyst surfaces under reaction conditions, rather than occurring in isolated distribution without mutual interaction. It has been demonstrated that reactants interact with reaction intermediates to enable a reaction to proceed (*1–4*). Thus it is important to know the behavior of intermediates under reaction conditions in order to understand the mechanism of catalytic reactions. Even when an intermediate is stable and does not react any further by itself, it is possible for a reaction to proceed catalytically through the same intermediate by an intermediate–reactant interaction (*1*).

It has been reported that the intermediate of the water–gas shift reaction ($CO + H_2O \rightarrow CO_2 + H_2$; WGSR) on the MgO surface is surface formate and that its rate-determining step is the decomposition of surface formate (*5, 6*). However, the WGSR has been observed not to proceed by the decomposition of surface formate made from CO and hydroxyl groups on MgO (*7*). This contradiction may be explained by either or both of the following two possibilities: (1) the surface formate made from surface OH and CO is not the intermediate of catalytic WGSR, and (2) WGSR does not proceed merely by the unimolecular decomposition of surface formate.

As the local structures of OH groups on MgO have been characterized in detail by FT–IR (*8*), it is possible on the well-characterized surface to spectroscopically discriminate the reactivities of different OH groups with CO and to explore the subsequent decomposition of the formates produced with different characteristics in the absence or presence of H_2O as a reactant. We may find factors important for catalytically promoting the WGSR by measuring the dynamic behavior of formate intermediate by *in situ* IR spectroscopy.

In this paper, we report on (1) OH groups active in producing surface formates; (2) structure and thermal stability of surface

0021-9517/90 $3.00

formates derived from CO and OH groups; (3) formate–water interaction; and (4) reaction mechanisms of the WGSR based on the local structures of active sites and an intermediate–reactant interaction.

EXPERIMENTAL

MgO powder was obtained by the thermal decomposition of $Mg(OH)_2$, which was made by the precipitation of $Mg(NO_3)_2$ (99%) with NH_3 (aq). $Mg(OH)_2$ powder was heated under vacuum at a rate of 3.3 K min^{-1} to 673 K and kept at this temperature for 3 h. The surface area was calculated to be 200 m^2 g^{-1} by BET measurements of N_2 adsorption. Commercially obtained CO gas (99.99%), D_2 gas (99.99%), and D_2O (99%) were used after repeated freeze–pump–thaw purification cycles.

Preparation of sample disks and pretreatment conditions are described in a previous paper (*8*). IR spectra were recorded on a JEOL JIR-10 Fourier-transform infrared spectrometer in the double beam mode using a liquid nitrogen-cooled MCT detector. The measurements were performed at room temperature or at reaction temperatures adding 200–400 scans at a 2-cm^{-1} resolution.

RESULTS

1. IR Absorption Bands of Surface Formates Formed from CO and Surface Hydroxyl Groups on MgO

Figures 1 and 2 show IR spectra of surface formates which were produced from CO and surface OD groups on MgO. The background absorption has been subtracted in each spectrum. Figure 1 shows the change in IR spectra when CO was admitted to the MgO sample at given temperatures. When CO was introduced at 320 K, bands at 2150, 1635, and 1284 cm^{-1} were observed. At 420 K new bands appeared at 2120, 1615, and 1321 cm^{-1}. By an additional introduction of CO at 470 K, new bands developed at ca. 2030, 1603, and 1358 cm^{-1}.

Figure 2 shows the change in IR spectra for surface formates by evacuation for 30 min at given temperature after the formation of surface formates at 523 K. The intensity of the peaks decreased after evacuating at 553–623 K, suggesting the decomposition of the surface formates in this temperature range. At first, the peaks of 2150, 1635, and 1280 cm^{-1} disappeared at 550 K, followed by a decrease in peak intensities at ca. 2030, 1603, and 1358 cm^{-1} and at 2120, 1615, and 1321 cm^{-1} above 550 K.

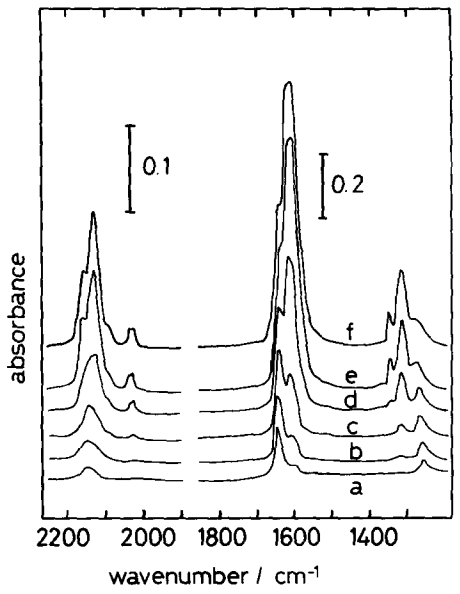

FIG. 1. IR spectra of surface formates ($DCOO^-$) on MgO. The sample was evacuated at 673 K, followed by exposure to CO ($P_{CO} = 5.53 \times 10^3$ Pa) for 30 min at (a) 323 K, (b) 373 K, (c) 423 K, (d) 473 K, (e) 523 K, (f) 573 K.

Bands observed at 2000–2150 cm^{-1}, 1600–1640 cm^{-1}, and 1280–1360 cm^{-1} are attributed to CD stretching (ν(CD)), OCO asymmetric stretching (ν_{as}(OCO)), and OCO symmetric stretching (ν_s(OCO)) of formate, respectively. In addition to these strong absorption bands, CH or CD out-of-plane bending and OCO in-plane bending peaks were observed at 1112 and 771 cm^{-1} for $HCOO^-$ species and at 900 and 767 cm^{-1} for $DCOO^-$ species. The peaks at 2150 (ν(CD)), 1635(ν_{as}(OCO)), and 1284 cm^{-1} (ν_s(OCO)) behaved in a similar way during

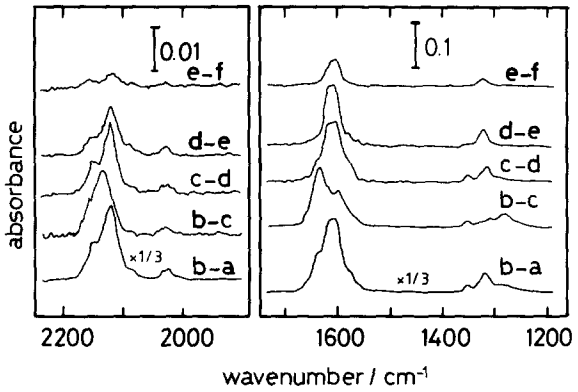

FIG. 2. Difference spectra between two of the following spectra: (a) evacuation at 673 K; (b) after a, CO introduction at 523 K (P_{CO} = 6.65 × 10^3 Pa); after b evacuation at (c) 553 K, (d) 573 K, (e) 593 K, and (f) 623 K. Each spectrum shows the decomposition of surface formate during two temperature changes.

various treatments. The three peaks at ca. 2030, 1603, and 1358 cm^{-1} and the three peaks at 2120, 1615, and 1321 cm^{-1} also behaved similarly. Careful measurements of the ca. 2030-cm^{-1} peak suggested the presence of two split peaks at 2035 and 2025 cm^{-1}. This was confirmed by the following experiment: Only the OH groups on top (terminal) of Mg_{3C} (3C indicates 3-coordination) were exchanged with D_2; the remaining OH groups on top of Mg_{4C} were not exchanged (*8*). The OD groups obtained were in contact with CO to form surface formates which showed a single peak at 2035 cm^{-1}. Therefore the peaks at 2035 and 2025 cm^{-1} are suggested to be due to CD stretching vibrations of the formates coordinated to Mg_{3C} and Mg_{4C}, respectively. Thus three kinds of surface formates, designated α, β, and γ, are indicated as being formed on the MgO surface. The ratio of these three formates is α-formate : β-formate : γ-formate ≃ 3 : 1 : 12 at temperatures higher than 450 K. The majority of formates exist as γ-formate on the MgO surface. Figure 3 shows the change in ν(CD) peaks as a function of reaction time in the formation of formates by the reaction of CO with surface OH groups on MgO pretreated at 673 K. The absorption bands and activation energies of formation and decomposition of the formates are listed in Table 1.

2. *Active Hydroxyl Group for the Reaction with CO*

In a previous paper (*8*), we distinguished six kinds of hydroxyl groups on MgO and

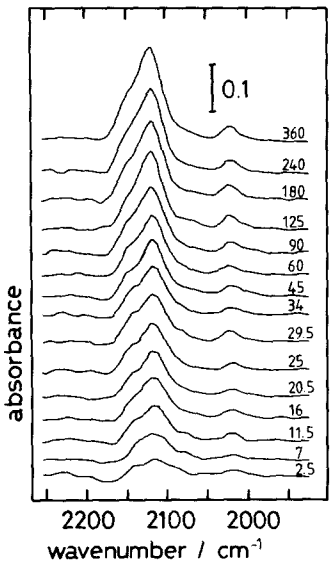

FIG. 3. Change in ν(CD) peaks of surface formate ($DCOO^-$) produced by the reaction of CO and OD groups at 523 K as a function of reaction time (in min). MgO, pretreated at 673 K; CO, 4.00 × 10^3 Pa.

TABLE 1

Absorption Bands[a] and Activation Energies for the Formation and Decomposition of Three Kinds of Formates on the MgO Surface

Type of formate	ν(CH) (cm^{-1})	ν_{as}(OCO) (cm^{-1})	ν_s(OCO) (cm^{-1})	E_a of formation[b] (kJ mol^{-1})	E_a of decomposition[c] (kJ mol^{-1})
α-formate (unidentate)[d]	2811(2150)	1649(1635)	1304(1284)	12.4 ± .3	89 ± 22
β-formate (bidentate)[d]	2750(2035) 2715(2025)	1610(1603)	1388(1358)	—	151 ± 19
γ-formate (bridge)[d]	2839(2120)	1622(1615)	1342(1321)	32.9 ± .9	159 ± 5

[a] Wavenumber for H-formate (D-formate).
[b] Obtained at 319–423 K.
[c] Obtained at 543–603 K.
[d] The assignment is described under Discussion.

showed that the reactivities of hydroxyl groups for the hydrogen exchange reaction with hydrogen molecules depend on their local structures. In this work, we investigated the reactivity of hydroxyl groups to produce surface formate. Figures 4a and 4b show the difference spectra before and after CO admission. The intensity of the peaks at 2765 and 2756 cm^{-1}, which are assigned to the on-top deuteroxyl groups (OD groups on Mg ions), decreased, while a broad band appeared at 2725 cm^{-1}. This broad peak may be due to on-top OD groups hydrogen-bonded with the produced formate, their peak intensities often being enhanced (*9*). Hence the decrease in peak intensity of the on-top OD groups observed in Fig. 4 (difference spectrum of b − a) involves both the reaction with CO and hydrogen bonding with the formates.

We examined the decomposition of surface formates (backward reaction) under vacuum as follows; at first the active OD groups were converted to surface formates by the reaction with CO at 523 K. Second, water vapor was introduced to change the

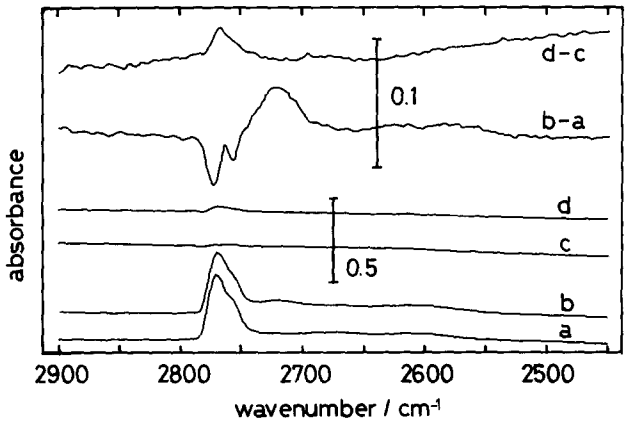

FIG. 4. ν(OD) stretching peaks of OD groups on MgO. (a) Evacuation at 673 K; (b) CO exposure at 523 K ($P_{CO} = 6.55 \times 10^3$ Pa); (c) after b, the sample was evacuated and then exposed to 400 Pa of H_2O at 323 K; (d) after c, evacuation at 673 K.

remaining OD groups to OH groups. By this treatment the deuterium of surface formate was not subjected to exchange with hydrogen from water. Finally, the formates were decomposed to OD and CO at 673 K under vacuum. A typical result is shown in Fig. 4 (difference spectrum d − c) which shows a peak at 2765 cm^{-1} with a shoulder at 2756 cm^{-1}. These bands are attributed to OD–Mg_{4C} and OD–Mg_{3C}, respectively, as described in the previous report (*8*). The ratio of the peak intensities of 2765 and 2756 cm^{-1} in Fig. 4 (d − c) was almost proportional to the ratio of the amount of OD–Mg_{4C} and OD–Mg_{3C}, suggesting that the reactivities of OD–Mg_{4C} and OD–Mg_{3C} with CO are similar and also that the formates produced are decomposed to the original OD groups.

When CO was introduced after OH–Mg_{3C} was converted to OD–Mg_{3C} by exchange with D_2 at 400 K followed by reaction with CO at 523 K, three ν(CD) bands appeared at 2150, 2035, and 2120 cm^{-1} for the CD stretching modes of α, β, and γ formates. This shows that α, β, and γ formates can be produced at the same site.

Next we investigated the ^{16}O–^{18}O exchange in the O atoms of hydroxyl groups in order to examine the reversible reaction between hydroxyl groups and formates. The ^{16}OD–Mg_{4C} peak at 2765 cm^{-1} and the ^{16}OD–Mg_{3C} peak at 2756 cm^{-1} for the sample evacuated at 673 K decreased when $C^{18}O$ was introduced at 523 K and new bands appeared at 2746 and 2738 cm^{-1} corresponding to ^{18}OD–Mg_{4C} and ^{18}OD–Mg_{3C}, respectively (Fig. 5). This result shows that the O atoms of hydroxyl groups can be exchanged with the O atoms of CO under the conditions where surface formates are formed.

3. Interaction between Surface Formate and Water

Figure 6a shows a TPD spectrum of surface formates ($DCOO^-$) made by introducing CO onto MgO at 520 K; Fig. 6b is a TPD spectrum of surface formates coadsorbed with water (after surface formates were produced at 520 K, the sample was exposed to water vapor at 470 K). In Fig. 6a the only desorbed product was CO, which showed a desorption peak at 560 K. On the other hand, the TPD spectrum of formates coadsorbed with water in Fig. 6b exhibits the evolution of CO and CO_2 at 620 K in addition to a broad peak at 520 K for D_2O. When water alone adsorbs on the MgO surface, the desorption peak appears at 490 K.

Table 2 shows the rate constants for the decomposition of surface formates with and without coadsorbed water. It should be noted that k_+ for the decomposition of H_2 +

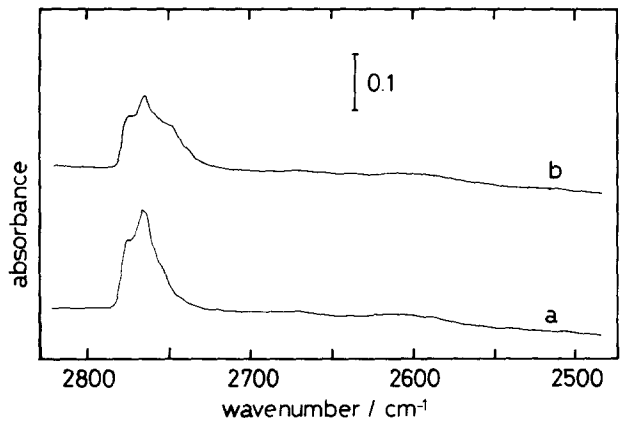

FIG. 5. IR spectra of OD groups on MgO, after (a) evacuation at 673 K; and (b) introduction of $C^{18}O$ at 523 K (P_{CO} = 6.55 × 10^3 Pa) followed by evacuation at 673 K.

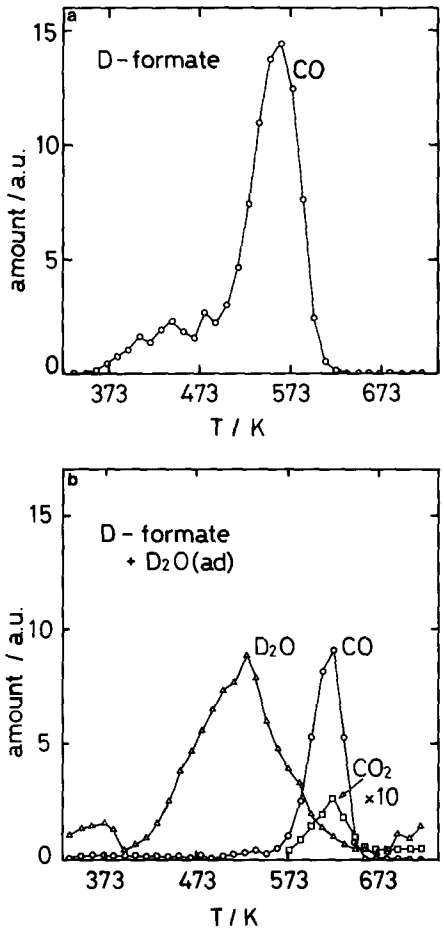

FIG. 6. (a) TPD spectrum of surface formate ($DCOO^-$) on MgO at a heating rate of 3.0 K min^{-1}; the surface formates were produced by the reaction of CD and OH groups at 520 K. (b) TPD spectrum (3.0 K min^{-1}) of surface formate ($DCOO^-$) coadsorbed with water on MgO; the surface formates were produced similarly to those in a, followed by the adsorption of water at 470 K. (△) D_2O, (○) CO, and (□) CO_2.

CO_2 was zero in the absence of water, whereas in the presence of water, the formation of H_2 and CO_2 was observed (k_+ is not zero); k_- for the decomposition to OH and CO became 10 times smaller than that without water.

Figure 7 shows the change in formate ($DCOO^-$) peaks caused by the introduction of water vapor. In the region of ν(CD), the two peaks at 2150 and 2120 cm^{-1} became a single peak at 2130 cm^{-1}, and the double

TABLE 2

Rate Constant for the Decomposition of Surface Formate as a Function of P_{H_2O}[a]

P_{H_2O} (Pa)	k_+ (10^{-4} s^{-1}[b])	k_- (10^{-4} s^{-1}[c])	k_+ ($k_+ + k_-$)
0	0	13	0
67	1.1	1.9	0.37
670	1.4	0.5	0.74

[a] Decomposition rate constants were measured at 600 K.

[b] k_+ is the rate constant for the decomposition of surface formates to CO_2 and H_2.

[c] k_- is the rate constant for the decomposition of surface formates to CO and surface OH.

peaks at 2035 and 2025 cm^{-1} became one peak of 2028 cm^{-1} (Fig. 7b). On evacuation at 630 K, the band at 2130 cm^{-1} shifted to 2120 cm^{-1} and the band at 2028 cm^{-1} split again into two bands at 2035 and 2025 cm^{-1}. In the OCO asymmetric stretching region, the intensity of the 1635-cm^{-1} peak was decreased by adsorption of water and the band at 1615 cm^{-1} shifted to 1593 cm^{-1}, becoming sharp. By evacuation of water, this

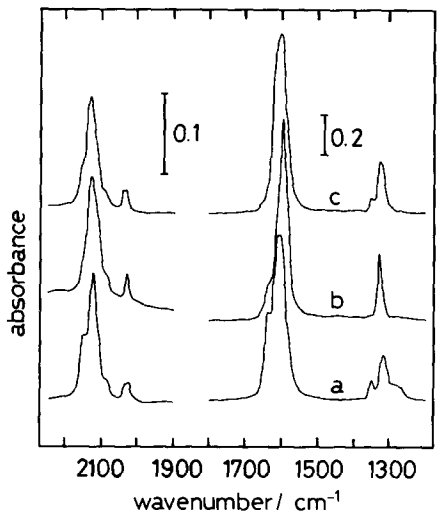

FIG. 7. Effects of adsorbed water of IR spectra of surface formates ($DCOO^-$) after evacuation of MgO at 673 K (a) exposed to CO at 573 K (P_{CO} = 6.65 × 10^3 Pa); (b) after a, exposed to D_2O vapor at 493 K (P_{D_2O} ≈ 400 Pa); (c) after b, evacuated at 630 K.

peak shifted to 1615 cm^{-1}, no peak at 1635 cm^{-1} being observed. In the OCO symmetric stretching region, the bands at 1358 and 1284 cm^{-1} almost disappeared and the peak at 1321 cm^{-1} shifted to 1333 cm^{-1} (Fig. 7b). The positions of the bands which were observed by evacuation after introduction of water were the same as the peak positions of the bands of β- and γ-formates. Furthermore, the formates characterized by those bands were decomposed at the same rate as γ- and β-formates at various temperatures. Thus the formates present at the MgO surface after water adsorption followed by evacuation are γ- and β-formates.

In the case of H-formate, ν_s(CO) values of β- and γ-formate became closer by the introduction of water; ν_s(OCO) of β-formate shifted from 1388 to 1381 cm^{-1}, while ν_s(OCO) of γ-formate shifted from 1342 to 1362 cm^{-1}.

Figure 8 shows the rate constants for the decomposition of surface formates as a function of temperature. The rate constant

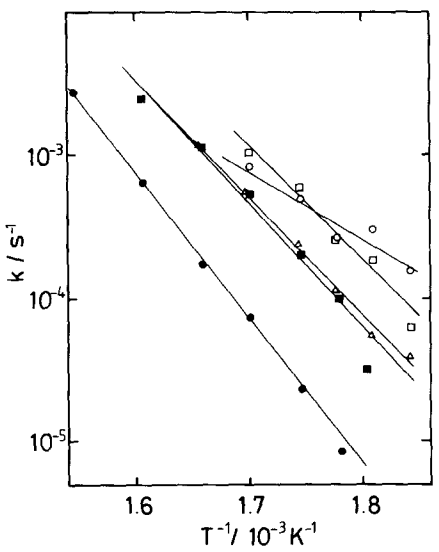

FIG. 8. Arrhenius plots for the decomposition of surface formates ($DCOO^-$) on MgO. (○) In the absence of water, (□) α-formate, (△) β-formate, (■) γ-formate; (●) formate produced by the introduction of water followed by evacuation was the same formate as cq, but coexisting with 133 Pa of water.

TABLE 3

IR Bands and Decomposition Rate Constants of γ-Formate in the Presence of Electron Donating Molecules[a]

Molecules	ν(CD)[b]	ν_{as}(OCO)[b]	ν_s(OCO)[b]	k_+[c]	k_-[c]
None	2120	1615	1321	0	13
Water	2130	1593	1333	1.4	0.5
Methanol	2125	1600	1334	0.5	7
Pyridine	2121	1595	1334	0	12
THF	2120	1610	1330	0	13

[a] The decomposition rate constants were measured at 600 K.
[b] In cm^{-1}.
[c] In 10^{-4} s^{-1}.

for the decomposition of surface formates in the presence of water is about 10 times smaller than that without water. The activation energy for the decomposition in the presence of water is 198 kJ mol^{-1}, which is larger by 40 kJ mol^{-1} than that in the absence of water.

Table 3 shows the absorption bands and decomposition rate constants of γ-formate in the presence of water, methanol, pyridine, and tetrahydrofuran (THF). ν_{as}(OCO) and ν_s(OCO) were observed to shift in the presence of these electron-donating compounds. The shift of ν(CD) was much less. The values k_+ and k_- were affected most by water, and methanol had less of an effect on the reaction. On the other hand, pyridine, which is a relatively strong donor, had no effect on k_+ and k_-. The transformation of α formate to γ formate occurred when water and methanol were introduced.

4. Comparison of the Rate of Formate Decomposition with the Rate of the Water–Gas Shift Reaction at Steady State

While the surface formates are stabilized by interaction with water as shown in Fig. 6, the formates are produced at temperatures much lower than those of their decomposition independent of the presence of water. Hence, the rate-determining step for the catalytic WGSR must be the decomposition of the formates. We examined

whether formate is an intermediate by comparing the decomposition rate of the stabilized formates with the rate of WGSR at steady state. The reaction rate (r_{calc}) is calculated by the equation

$$r_{calc} = k \times M \times R, \quad (1)$$

where k is the rate constant for the decomposition of formates which is obtained from the decrease in IR peak intensity, R represents the ratio of CO_2 formed to all formates decomposed, and M is the amount of surface formate. After measurement of the reaction rate at steady state (r_{obs}), the gas phase was evacuated for 1 min and the rate constants for the formation of CO_2 (k_+) and of CO (k_-) were determined. Thus the selectivity (R) in the decomposition of formates at the same concentration as that at steady state can be obtained. The value R is calculated by the equation

$$R = k_+/(k_+ + k_-). \quad (2)$$

Table 4 shows the results. The reaction rates calculated from the decomposition of surface formates are in good agreement with the reaction rates at steady state. The values of ($k_+ + k_-$) are almost the same as the decomposition rates of formates obtained from the decrease in IR peak intensity. Thus it may be concluded that the formate observed in IR spectra is the intermediate of the catalytic WGSR.

TABLE 4

Comparison of Calculated and Observed Values of the Water–Gas Shift Reaction[a]

T (K)	P_{H_2O} (10^3 Pa)	P_{CO} (10^3 Pa)	M (mol kg^{-1})	R	k (10^{-5} s^{-1})	r_{calc}[b]	r_{obs}[b]
580	0.67	1.33	0.046	0.69	4.8	1.5	1.3
590	0.67	1.33	0.039	0.71	7.1	2.0	2.2
610	0.67	1.33	0.026	0.70	29	5.3	4.8
610	0.07	1.33	0.023	0.35	46	3.7	3.4
610	0.67	0.67	0.012	0.84	29	2.9	3.1
610	0.67	4.00	0.050	0.76	29	7.3	7.2

[a] M, R, and k represent the amount of formate under reaction conditions, the ratio of CO_2 to decomposed formate, and the rate constant for the decomposition of formates in the presence of water, respectively.

[b] r_{calc} represents the rate of WGSR calculated from Eq. (1), and r_{obs} represents the observed reaction rate. The unit is 10^{-6} mol s^{-1} kg^{-1}.

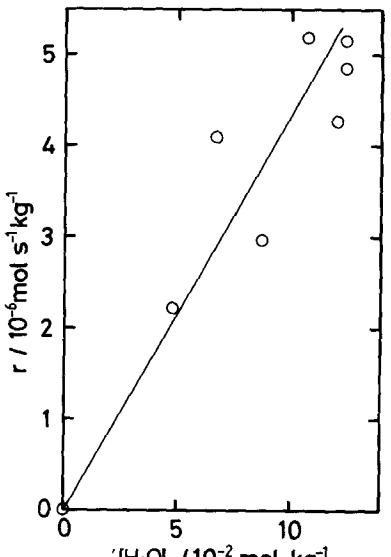

FIG. 9. Rate (r) of WGSR at steady state as a function of the amount of adsorbed water $[H_2O]_{ad}$; T = 603 K, $P_{CO} = 1.33 \times 10^3$ Pa.

The apparent activation energy of WGSR was found to be 175 ± 9 kJ mol^{-1}, which is lower by ca. 20 kJ mol^{-1} than that for the decomposition of surface formates in the presence of water (195 ± 5 kJ mol^{-1}). The ratio R is almost constant at various temperatures, and M gets smaller as the temperature increases. Thus the temperature dependence of R should be smaller than that of k.

Figure 9 shows the reaction rate as a function of the amount of adsorbed water. The reaction rate was found to be proportional to the amount of adsorbed water.

Table 5 shows the rate constant of CO_2 formation in the system of formate ($HCOO^-$ or $DCOO^-$) and water (H_2O or D_2O). The isotope effect was observed when $HCOO^-$ was replaced by $DCOO^-$, but it was not observed with water molecules. The rate of CO_2 formation from $HCOO^-$ + water is ca. 1.5 times faster than that from $DCOO^-$ + water.

TABLE 5

Rate Constant for CO_2 Formation (k_+) in Various Combinations of Labeled Water and Formate[a]

Combination	k_+ (10^{-5} s^{-1})
$HCOO^- + H_2O$	6.3
$HCOO^- + D_2O$	5.8
$DCOO^- + H_2O$	4.0
$DCOO^- + D_2O$	4.0

[a] The decomposition rate constants were measured at 580 K.

DISCUSSION

1. *Assignment of Three Kinds of Surface Formates*

Three kinds of surface formates, α, β, and γ, were produced by the reaction of CO and OH groups on the MgO surface. The structure of each formate can be determined by the value of $\Delta\nu = \nu_{as}(OCO) - \nu_s(OCO)$ (*10*). When $\Delta\nu$ is larger or smaller than that of a free ion, the formate is considered to be unidentate or bidentate, respectively. When $\Delta\nu$ is as large as that of a free ion, it is assigned the bridge-type structure (*10*). The structures and OCO stretching frequencies of several metal formate complexes have been reported. Formate types $\nu_{as}(OCO)$, $\nu_s(OCO)$, and $\Delta\nu$ are listed in Table 6. The values of $\Delta\nu$ for the bridge-type formate are in the range of ca. 220–280 cm^{-1}, and those of unidentate- and bidentate-type formates are larger than 300 cm^{-1} and around 200 cm^{-1}, respectively. Thus α-formate in Table 1 is straightforwardly assigned a unidentate-type structure; again, γ-formate is undoubtedly bridge type. There are two possibilities for the assignment of β-formate from the value of $\Delta\nu$ in Table 1; either it is bidentate or it is bridge type. Because all three kinds of formates are produced at the same site (OD–Mg_{3C}), it is unlikely that both β- and γ-formates are bridge type. Consequently, α, β-, and γ-formates are suggested to have unidentate, bidentate, and bridge structures, respectively, as given in Table 1.

The presence of bidentate formate is supported by the fact that ^{18}OD was formed on production of surface formates from ^{16}OD and $C^{18}O$. In the decomposition of bridge-type formate in the absence of water, the same hydroxyl groups that existed before the reaction with CO are recovered, and the exchange of O atoms between hydroxyl

TABLE 6

Carboxyl Stretching Frequencies and Structures of Formates

Compound	$\nu_{as}(OCO)$	$\nu_s(OCO)$	$\Delta\nu$[a]	Structure	Ref.
$Be(HCOO)_2(NH_3)_2$	1700	1337	330	Unidentate	*16*
	~1590	~1293	(ave.)		
$C(H_gOCOH)_4$	1677	1360	317	Unidentate	*17*
$Be(HCOO)_2$	1619	1410	209	Bidentate	*18*
$UO_2(OOCH)_2 \cdot H_2O$	1560	1360	200	Bidentate	*19*
$[Cr_3O(OOCH)_6(H_2O)_3]$	1654	1378	270	Bridge	*20*
	1640	1370	(ave.)		
$[Cr_3O(OOCH)_6(py)_3]$	1635	1370	275	Bridge	*20*
	1655		(ave.)		
$[Cr_3O(OOCH)_6(\gamma\text{-pic})_3]$	1635	1370	275	Bridge	*20*
	1655		(ave.)		
$[Fe_3O(OOCH)_6(H_2O)_3]$	1620	1370	250	Bridge	*20*
$Be_4O(OOCH)_4$	1637	1422	215	Bridge	*21*
$(m\text{–}H)(m\text{–}O_2CH)Os_3(CO)_{10}$	1576	1362	214	Bridge	*22*

[a] In cm^{-1}.

groups and CO does not occur through bridge-type formates. But oxygen exchange is possible when it proceeds through bidentate formates, as is the case of the present result. As the amount of exchanged O atoms in hydroxyl groups was much larger than the quantity of β-formates, the three kinds of formates are suggested to be in equilibrium. It should be noted that the unidentate formate is the first surface formate produced at low temperatures, followed by bidentate and bridged formates with increasing temperature as shown in Fig. 1. The unidentate formate was preferably converted to the bridged formate in the presence of water.

The OH groups on an ideal MgO(001) flat surface are known to be unstable and readily removed by evacuation at 673 K (*11*), the temperature at which the samples were usually pretreated. Therefore, most of the OH groups remaining after pretreatment of MgO may be located on coordinatively unsaturated sites such as step and kink sites. Neighboring coordinatively unsaturated Mg atoms are necessary to form bridge-type formates which are the main species under catalytic reaction conditions.

2. *Interaction between Surface Formate and Water*

(2) *Conversion of unidentate-type formate to bridge-type formate.* The conversion of unidentate-type to bridge-type formate by the introduction of water is shown in Fig. 7. The conversion required a heating to more than 450 K, indicating that the structural transformation is an activated process. On the other hand, the bands of bridge- and bidentate-type formates were shifted immediately by exposure to water vapor at room temperature; the shift is due to the interaction with water molecules and not to structural transformations. The amount of bridge-type formate is much greater than that of bidentate formate, particularly in the presence of water, and most surface formates exist as bridge type under WGSR conditions. Electron-donating compounds gave formate peak shifts similar to those of the case of water as sown in Table 3. These donors adsorb on coordinatively vacant sites on Mg cations. The interaction with water is shown in Fig. 10, and is discussed later.

(2) *Stabilization of surface formates.* Surface formates were stabilized by the presence of water as revealed in Fig. 6, which shows an upward shift in the TPD peak. The rate constant k_- for the decomposition of formates is more than 10 times smaller than that in the absence of water. In the TPD spectrum of Fig. 6b the desorption peak of water is observed at 520 K, while a sharp peak of CO appears at 620 K. As most of the water molecules have desorbed at WGSR temperatures in the TPD measurement, most of the surface formates are decomposed into OH groups and CO as shown in Fig. 6b. Under catalytic WGSR conditions where water is present in the gas phase, 70% of surface formates are decomposed into CO_2 and H_2.

Water molecules are also stabilized by surface formates. Without surface formates, a desorption peak appears at 490 K in the TPD spectra; on the other hand, a desorption peak appears at 520 K when they coadsorb with formates. As the reaction temperature is ca. 100 K higher than these temperatures, however, the amount of physisorbed water does not change drastically with or without surface formates at reaction temperatures.

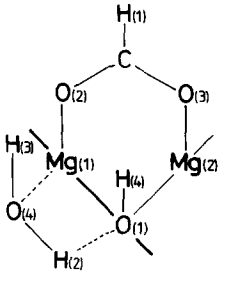

FIG. 10. A proposed structure for coadsorption of bridge formate and water on reaction sites.

(3) Creation of the reaction path toward CO_2 and H_2. As a large number of hydroxyl groups exist on the MgO surface, it is thermodynamically possible for surface formates to decompose both to $CO_2 + H_2$ and to CO + OH. However, the decomposition to $CO_2 + H_2$ was never observed, as shown in Table 2, 100% of the surface formate being decomposed to CO and OH. The introduction of water increased the total quantity of OH groups + adsorbed water only two to three times at reaction temperatures. The decomposition is kinetically controlled, not controlled by thermodynamical equilibrium. Thus these results show that adsorbed water molecules create a reaction channel for the dehydrogenation of surface formates to form CO_2 and H_2. The activation energy of k_+ for the forward decomposition in the presence of water is similar to that of k_-. Surface Mg and O ions on the reaction sites are always terminated with formate or OH groups and bare surface ions are not formed during WGSR because the decomposition of formates to CO_2 and H_2 is accompanied by the dissociation of H_2O.

(4) Effect of adsorbed water on vibrational modes of surface formates and rate constants. The difference in the local structure of reaction sites is caused by the difference in the degree of coordination unsaturation. The two bands for ν(CD) of β-formate (2035 and 2025 cm^{-1}) are due to the difference in site structures as described above. The split peaks joined to become a single peak at 2028 cm^{-1} when water was introduced. The ν_{as}(OCO) peak also became sharper, changing from 35 to 15 cm^{-1} FWHM, with the introduction of water. Water adsorbed at coordinatively unsaturated sites as shown in Fig. 10, decreasing site differences and instigating the change of the double ν(CD) peak to the single peak. The two ν(CD) peaks at 2025 and 2035 cm^{-1} also changed to one band at 2025 cm^{-1} by the introduction of pyridine or THF. Again, ν_{as}(OCO) and ν_s(OCO) values of bridge-type formates shifted in a way similar to the case of water. This suggests that water molecules behave as electron donors toward coordinatively unsaturated Mg ions.

On the other hand, pyridine and THF did not change the values of k_+ and k_-; that is, these electron donors did not promote the forward reaction to form CO_2 and H_2. However, effects on rate constants and peak shifts similar to those of water were observed with methanol, which is a weak electron donor, but can hydrogen-bond with O anions on the MgO surface. As a common feature of water and methanol in adsorption, a coadsorption structure involved in WGSR is shown in Fig. 10, where the water molecule donates electrons to the Mg ion by the lone-pair electron of the oxygen atom and withdraws electrons from the lattice oxygen atom with the hydrogen atom.

The 3*s* orbital of Mg ions on a MgO(001) flat surface is concealed by the 2*p* orbital of the adjacent O ions. When the O ion forms a chemical bond with a H^+ ion, however, the 2*p* orbital of the O ion is localized at the O–H bond to make a σ bond and its energy level decreases. As a result, the 3*s* orbital of the adjacent Mg ion appears at the surface and its energy level rises (*12*). Thus the energy level of the 3*s* orbital of Mg(2) in Fig. 10 is increased by the coordination of H(2) to O(1), making it easier for a chemical bond to form between Mg(2) and O(3) in Fig. 10. Both electron donation and electron withdrawal between a MgO pair and a H_2O molecule are important in the conversion of unidentate formate to bridge formate, the decrease in k_-, and the promotion of the forward decomposition of surface formates.

3. *Reaction Mechanism for the Water–Gas Shift Reaction*

The rate constants for the forward decomposition of bridge formates at the same surface concentration as that at steady state were in agreement with the rate constants for steady state WGSR under variations conditions as shown in Table 4. The major-

ity of surface formates under reaction conditions were of the bridge type as mentioned above. The bridge formate itself was not decomposed to CO_2 and H_2, and the interaction with adsorbed water in Fig. 10 was necessary for the reaction to proceed as shown in Table 2 and Fig. 9. Thus the bridge-type formate is a primary intermediate of WGSR and its decomposition in the presence of water is the rate-determining step.

It has been reported that CO_2 adsorbs strongly on the MgO surface evacuated above ca. 1000 K (*13–15*). On the sample evacuated at 673 K, however, a CO_2 desorption peak appeared at 523 K, which is lower than the reaction temperature. IR absorption bands attributed to CO_2 adsorption were not detected under the WGSR conditions. These results exclude the possibility that the rate-determining step is the desorption of CO_2.

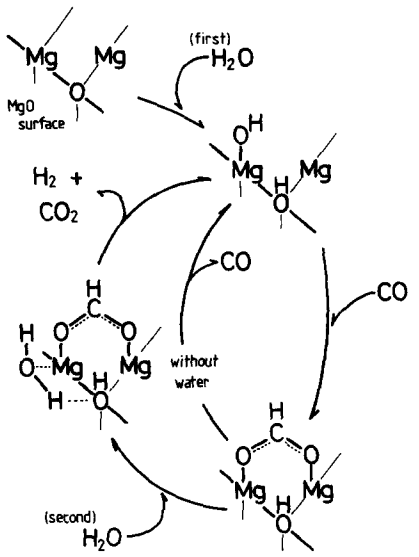

SCHEME 1. A reaction mechanism for the water–gas shift reaction on MgO.

Under catalytic reaction conditions small amounts of bidentate-type formate exist in addition to bridge-type formate. Because the catalytic reaction rate agrees with the decomposition rate of bridge-type formate in the presence of water, bidentate formate cannot have a higher reactivity than bridge-type formate. The peak shifts of β-formate caused by water adsorption are not as large as those of γ-formate, suggesting a relatively weak interaction between them. Furthermore, for stereochemical reasons, water cannot coordinate to Mg_{4C} sites with ligands; it can only coordinate to Mg_{3C} sites. Very little bidentate formate seems to occur on Mg_{3C} sites, judging from the IR data. Thus the bidentate formate may not be an important intermediate for WGSR on the MgO surface.

Scheme 1 shows the backward decomposition of the bridge formate and the catalytic cycle for WGSR. Water dissociates preferably at edge or corner sites on the MgO surface to produce on-top and bridge hydroxyl groups. CO reacts with the on-top OH groups to produce surface formates as proved by IR. The rate of the formation of surface formates is $>7 \times 10^{-5}$ mol kg^{-1} s^{-1} at 580 K, which is more than 20 times faster than the rate of decomposition of the formate (2.2×10^{-6} mol kg^{-1} s^{-1} at 580 K). The formation of formates is not prevented by water. Almost all formates are of the bridge type under reaction conditions.

Surface formate decomposes into CO and OH in the absence of water. However, in the presence of water, 70% of the surface formates decompose to CO_2 and H_2. The reaction rate increased linearly with the amount of adsorbed water as shown in Fig. 9. Water coadsorbed with the formate remained on the surface at 600 K, whereas physisorbed water on the MgO surface desorbed immediately at the same temperature. Water molecules are suggested to interact more strongly with Mg sites coordinated by formates than with other Mg sites without formate ligands.

The most probable mechanism for the adsorption of water is shown in Fig. 10, where the electron-donating and -withdrawing characteristics of water molecules are essential for the forward decomposition of the formates to produce CO_2 and H_2 as dis-

cussed above. The interaction of water also prevents the backward decomposition of formates to CO and OH groups.

The isotope effect of the formate hydrogen on CO_2 formation was observed (Table 5), but no isotope effect was observed for the hydrogen of water or bridged OH. Thus the rate-determining step may involve the dissociation of the CH bond of the bridge formate in the transition state. The hydrogen produced in the $DCOO^- + OH (+H_2O)$ system was HD. There are two explanations for HD formation: (1) HD is formed from the formate deuterium and the bridge OH; and (2) HD is produced from the formate deuterium and the water hydrogen. We cannot, however, distinguish between these two possibilities because a rapid hydrogen exchange between water and bridge hydroxyl groups occurs. It is most likely from the stereochemical aspect (Fig. 10) that the water–formate complex decomposes in the following way: at/near the transition state, the delocalization of electrons through the O–C–O bond in the formate ($HCOO^-$) reduces the bond order to close to one, followed by rotation and torsion around C–O(2), C–O(3), and C–H(1) bonds; this leads to the interaction of H(1) with H(4) in Fig. 10. H(4) has δ_+ charge, while H(1) has δ_- character. The tilting of the bridge formate may promote the dissociation of the C–H(1) bond to form hydrogen (H(1)H(4)) with a concomitant formation of CO_2, accompanied by the dissociation of adsorbed water to form Mg(1)–O(4)H and O(1)–H(2) bonds. These reaction processes are not possible without the assistance of adsorbed water.

REFERENCES

1. Nishimura, M., Asakura, K., and Iwasawa, Y., *in* "Proceedings, 9th International Congress on Catalysis, Calgary, 1988" (M. J. Phillips and M. Ternan, Eds.), Vol. 4, p. 1842. Chem. Institute of Canada, Ottawa, 1988.
2. Cant, N. W., and Bell, A. T., *J. Catal.* **73,** 257 (1982).
3. Ueno, A., Onishi, T., and Tamaru, K., *Trans. Faraday Soc.* **67,** 3585 (1971).
4. Yamashita, K., Naito, S., and Tamaru, K., *J. Catal.* **94,** 353 (1985).
5. Scholten, J. J. F., Mars, P., Menon, P. G., and Hardereld, R. Van, *in* "Proceedings, 3rd International Congress on Catalysis, Amsterdam, 1964," Vol. 2, p. 881. Wiley, New York, 1965.
6. Ueno, A., Onishi, T., and Tamaru, K., *Trans. Faraday Soc.* **66,** 756 (1970).
7. Gopal, P. G., Schneider, R. L., and Watters, K. L., *J. Catal.* **105,** 366 (1987).
8. Shido, T., Asakura, K., and Iwasawa, Y., *J. Chem. Soc. Faraday Trans. 1* **85,** 441 (1989).
9. Little, L. H., "Infrared Spectra of Adsorbed Species." Academic Press, London, 1966.
10. Nakamoto, K., "Infrared and Raman Spectra of Inorganic and Coordination Compounds," 3rd ed. Wiley–Interscience, New York, 1987.
11. Onishi, H., Aruga, T., Egawa, C., and Iwasawa, Y., *Surf. Sci.* **191,** 479 (1987).
12. Tsukada, M., and Shima, N., *Shokubai* **29**(2), 102 (1987).
13. Evans, J. V., and Whateley, T. L., *Trans. Faraday Soc.* **63,** 2769 (1967).
14. Gregg, S. J., and Ramsay, J. D., *J. Chem. Soc. A,* 2784 (1970).
15. Fukuda, Y., and Tanabe, K., *Bull. Chem. Soc. Japan* **46,** 1616 (1973).
16. Grigor'ev, A. I., Donchenko, N. V., Dunaeva, K. M., and Debabov, D. V., *Zh. Neorg. Khim.* **30,** 888 (1985).
17. Mink, J., Meic, Z., Gal, M., and Korpar-Coliq, B., *J. Organomet. Chim.* **256,** 203 (1983).
18. Johnson, M. K., Powell, D. B., and Cannon, R. D., *Spectrochim. Acta Part A* **38**(2), 899 (1982).
19. Anan'ec, A. V., Bukhtiyarova, T. N., and Krot, N. N., *Radiokhimiya* **25**(3), 349 (1982).
20. Johnson, M. K., Powell, D. B., and Cannon, R. D., *Spectrochim. Acta Part A* **37**(11), 995 (1981).
21. Johnson, M. K., Powell, D. B., and Cannon, R. D., *Spectrochim. Acta Part A* **38**(2), 125 (1982).
22. Shapley, J. R., St. George, G. M., Churchill, M. R., and Hollander, F. J., *Inorg. Chim.* **21,** 3295 (1982).